Singlet Ground State of the Quantum Antiferromagnet $Ba_3CuSb_2O_9$

J. A. Quilliam,[1] F. Bert,[1] E. Kermarrec,[1] C. Payen,[2] C. Guillot-Deudon,[2] P. Bonville,[3] C. Baines,[4] H. Luetkens,[4] and P. Mendels[1,5]

[1]*Laboratoire de Physique des Solides, Université Paris-Sud 11, UMR CNRS 8502, 91405 Orsay, France*
[2]*Institut des Matériaux Jean Rouxel, UMR 6502 Université de Nantes, CNRS, 2 rue de la Houssinière, BP 32229, 44322 Nantes Cedex 3, France*
[3]*Service de Physique de lÉtat Condensé, CEA-CNRS, CE-Saclay, F-91191 Gif-Sur-Yvette, France*
[4]*Laboratory for Muon Spin Spectroscopy, Paul Scherrer Institute, CH-5232 Villigen PSI, Switzerland*
[5]*Institut Universitaire de France, 103 Boulevard Saint-Michel, F-75005 Paris, France*

(Received 8 June 2012; published 11 September 2012)

We present local probe results on the honeycomb lattice antiferromagnet $Ba_3CuSb_2O_9$. Muon spin relaxation measurements in a zero field down to 20 mK show unequivocally that there is a total absence of spin freezing in the ground state. Sb NMR measurements allow us to track the intrinsic susceptibility of the lattice, which shows a maximum at around 55 K and drops to zero in the low-temperature limit. The spin-lattice relaxation rate shows two characteristic energy scales, including a field-dependent crossover to exponential low-temperature behavior, implying gapped magnetic excitations.

DOI: 10.1103/PhysRevLett.109.117203 PACS numbers: 75.10.Kt, 76.60.−k, 76.75.+i

In recent years, the field of geometrically frustrated magnetism has been galvanized by the discovery of several promising candidates for quantum spin liquid (QSL) physics in kagome [1,2], hyperkagome [3] and triangular lattice [4,5] geometries. The most recent and surprising discoveries in this vein have come in the 6*H*-perovskite family, $Ba_3MSb_2O_9$ where M = Cu, Ni [6,7], and have generated an enormous theoretical interest [8–12].

Here we focus on the $S = 1/2$ antiferromagnet $Ba_3CuSb_2O_9$, originally thought to feature a triangular lattice of Cu^{2+} spins [13] and shown by Zhou *et al.* to exhibit a very surprising gapless QSL state [6] with a lack of static magnetism down to 200 mK, well below the Weiss temperature, $\theta_W \simeq 50$ K, and a peculiar linear specific heat. An in-depth characterization, including single crystals, of Nakatsuji *et al.* [14] on the other hand has shown that the structure more likely involves triangular bilayers equally occupied by Cu and Sb that form a decorated honeycomb lattice during crystal growth as a result of electric-dipole interactions between Sb^{5+}-Cu^{2+} 'dumbbells' that map onto a frustrated Ising model. Moreover, it has been shown that a crucial ingredient in the physics of $Ba_3CuSb_2O_9$ is the orbital degrees of freedom. The system is Jahn-Teller (JT) active, with three equivalent local distortions and corresponding $d_{x^2-y^2}$ orbitals. In some off-stoichiometric samples, a collective orthorhombic JT transition at ∼200 K occurs, whereas stoichiometric samples maintain hexagonal symmetry, show minimal anisotropy, and remain dynamic.

The lack of static magnetism in $Ba_3CuSb_2O_9$ to $T \ll \Theta_W \sim 50$ K remains a profound result. Neither triangular nor honeycomb nearest neighbor antiferromagnets are expected to have QSL ground states and apparent JT instabilities make it even more surprising. Two likely proposals have emerged: either a new type of QSL on the honeycomb lattice accompanied by dynamic JT distortions or a random singlet state (RSS) driven by static JT distortions on a rather disordered lattice [14,15]. An understanding of this system therefore hinges on a characterization of the ground state and the evolution of the susceptibility and spin fluctuations.

In this Letter, we have applied the local probe techniques, muon spin relaxation (μSR) and nuclear magnetic resonance (NMR), to $Ba_3CuSb_2O_9$. We demonstrate in this system a lack of static magnetism in zero-field, singlet formation around 50 K and a lower temperature field-induced gap. Our measurements help distinguish between the two possible scenarios proposed in Ref. [14] and favor a RSS.

The synthesis and structural characterization of the polycrystalline $Ba_3CuSb_2O_9$ samples studied in this work are described in the Supplemental Material [16]. Macroscopic susceptibility, χ_{macro}, measurements reveal a Weiss temperature, $\theta_W \simeq 51$ K, consistent with previous work [6,14] and Curie constant of 0.48 K emu/mol/Oe, implying either a somewhat large $g = 2.27(1)$ (relative to ESR results, $g = 2.20$ [14]) or else a 6% surplus of Cu. All characterization techniques employed [16] have revealed an Sb/Cu ratio stoichiometric to well within ±10% indicating [14] that our samples should maintain hexagonal symmetry.

To further confirm that our samples are consistent with the hexagonal phase of Ref. [14] and not the orthorhombic phase that exhibits freezing at $T_g = 100$ mK, we performed μSR experiments at PSI from 150 K down to 20 mK. The zero field (ZF) polarization of the bulk [17] can be fit at all temperatures with a static Kubo-Toyabe function with $\Delta H = 0.76 \pm 0.2$ G, resulting from nuclear

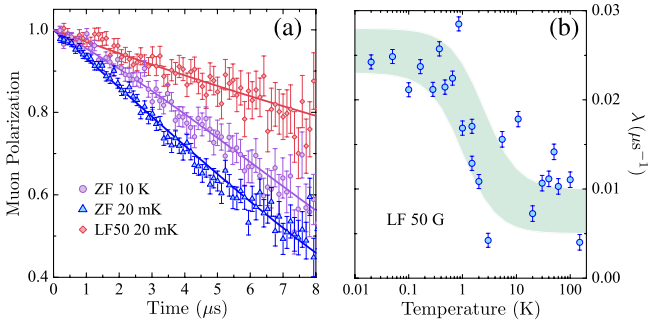

FIG. 1 (color online). (a) Muon polarization at $T = 10$ K in zero field and at $T = 20$ mK in zero field, and longitudinal field of 50 G. The fits are exponential relaxation, multiplied with a Kubo-Toyabe form of nuclear origin for the ZF data. (b) Relaxation rate $\lambda(T)$ in a longitudinal field of 50 G. The shaded region is a guide to the eye.

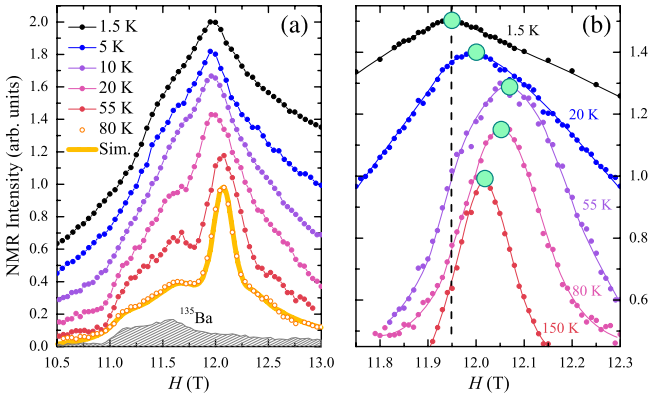

FIG. 2 (color online). (a) Selected ^{123}Sb NMR spectra, including a simulation of the spectrum at 80 K. The ^{135}Ba satellite can be isolated (shaded area) by roughly doubling the rf pulses. (b) Peak of spectra at several temperatures showing the nonmonotonic shift (large, green circles).

moments, and weak exponential relaxation of dynamical origin (see Fig. 1). The results show that there is a complete lack of spin freezing [18] in $Ba_3CuSb_2O_9$ down to 20 mK in ZF, in agreement with Ref. [14]. Applying a 50 G longitudinal field (LF) decouples the muons from the nuclear moments and reveals changes in spin dynamics. The relaxation rate, $\lambda(T)$, obtained through exponential fits [Fig. 1(b)], is very weak with a subtle increase as T is decreased and is comparable to that of herbertsmithite [1,19].

To precisely study the spin dynamics and in-field behavior of $Ba_3CuSb_2O_9$, we turn to a more strongly coupled probe: Sb NMR. Spectra are obtained with the standard $\pi/2$-τ-π pulse sequence ($14 < \tau < 23$ μs) and integration of the echo as the field is swept. Below 20 K, Cu NMR signals are seen, superimposed on the ^{121}Sb spectra. A ^{135}Ba quadrupolar satellite is found near the ^{123}Sb line, but is small and does not change in temperature. Hence, most of this work concentrates on ^{123}Sb. The high-temperature NMR spectra are consistent with a distribution of quadrupolar couplings, since the broadening of the quadrupolar satellites is larger than that of the central line. This can be seen to result from Cu-Sb dumbbell disorder inherent in the decorated honeycomb lattice and random JT distortions [14]. A powder simulation with parameters $\nu_Q \simeq 3.7 \pm 0.9$ MHz for the $I = 7/2$ ^{123}Sb nucleus is shown in Fig. 2. While there are two inequivalent Sb sites in the structure, they are not discernible in the spectra. The line shift, K, is obtained from the position of the maximum of each spectrum and is shown in Fig. 3. A scaling of K at high T with $\chi_{\rm macro}$ reveals a hyperfine coupling of $A = dK/d\chi_{\rm macro} \simeq 12$ kOe/μ_B and shows that the temperature-independent shift (which may be chemical and/or quadrupolar) is only ~80 ppm.

The most striking observation in the Sb NMR spectra is the nonmonotonic shift (intrinsic susceptibility), K ($\chi_{\rm int}$), shown in Fig. 3. The maximum in $\chi_{\rm int}$ is found at a remarkably high temperature ~55 K $\simeq \theta_W$. Clearly this material does not behave like a nearest-neighbor $S = 1/2$ triangular lattice antiferromagnet, as seen from comparison with the high-temperature series expansion [20], in Fig. 3. The appearance of strong spin correlations or dimerization at such a high temperature is unusual for a QSL and implies a lack of magnetic frustration.

Equally important is the observation that $\chi_{\rm int}$ drops out appreciably and appears to approach zero as $T \to 0$. We cannot, however, differentiate between an exponential (gapped excitations) or power-law (gapless excitations) limit with K given the sizable linewidth. $\chi_{\rm int}$ here contrasts heavily with behavior observed in other QSL candidates. For example the organic triangular lattice systems, which

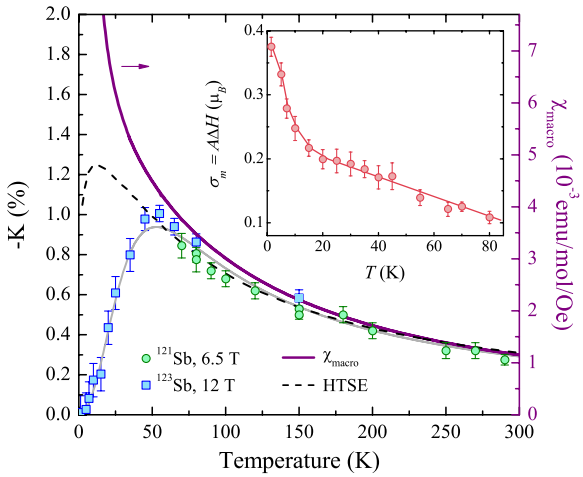

FIG. 3 (color online). Left axis: NMR line shift, K, taken with ^{121}Sb at 6.4 T (high T only) and ^{123}Sb at 12 T. Right axis: $\chi_{\rm macro}$ at 5 T minus diamagnetic susceptibility $\chi_{\rm dia} = -1 \times 10^{-4}$ emu/mol/Oe [14]. Also shown is the high-temperature series expansion of χ for the $S = 1/2$ triangular lattice antiferromagnet [20]. Inset: Standard deviation of local magnetization, $\sigma_m = A\Delta H$.

are thought to be described by a QSL model with a Fermi surface of spinons [21,22], exhibit finite susceptibility as $T \to 0$ [4,5].

Comparison with χ_{macro} (Fig. 3) illustrates the significant level of defect contribution in the system. Magnetization measurements at low T up to 14 T, show that ~16% of the spins in the system are weakly interacting with $\theta_{\text{def}} \simeq -0.5$ K at the lowest temperatures measured and are easily saturated with an applied magnetic field [16]. Note that the sample studied here displays the same size of Curie tail as in Refs. [6,14] suggesting that it might be an intrinsic property of the decorated honeycomb lattice. Although such a weakly coupled defect or 'orphan spin' [23] contribution is commonplace in related systems [24–28], here it seems likely that it originates from the out-of-plane Cu′ site which is inherent in the decorated honeycomb structure and is linked to the honeycomb motifs by a frustrated isosceles triangle (see the structure in Ref. [14]).

Meanwhile, the linewidth (shown in the inset of Fig. 3, obtained with Gaussian fits to parts of the spectra where the central line can be isolated) monotonically increases despite the drop in χ_{int}, implying that the linewidth is dominated by a defect-induced staggered magnetization or spin texture related to the Curie-tail. At low T, the linewidth surprisingly represents a significant fraction of the full moment (almost $0.4\mu_B$), despite zero line shift.

To assess the nature of the magnetic excitations, we turn to the spin-lattice relaxation rate, $1/T_1$. Because the recovery curves, $M(t)$, consist of multiple stretched exponentials [29], we have simply defined T_1 by the point where $1 - M(t)/M_\infty = 1/e$. The quadrupolar Sb nuclei are in principle sensitive to magnetic and charge fluctuations. Comparison of $1/T_1$ for the two Sb isotopes (with very different gyromagnetic ratios, γ, and quadrupolar moments, Q) at constant γH and $T > 20$ K, shows a ratio $^{123}T_1/^{121}T_1 \simeq 1.6$. This is close to the ratio 1.7 that we would expect if we were primarily probing magnetic fluctuations, rather than 0.6 which would be expected of charge fluctuations [29]. Thus, the JT distortions proposed in Ref. [14] are either fully static or dynamic on a time scale too fast for NMR.

The T-dependence of $1/T_1$, taken at fields of 6.5 T and 12 T is shown in Fig. 4 and shows three distinct regimes of relaxation. At high T, a small drop in $1/T_1$ is observed and in a plot of $\log(1/T_1)$ vs $1/T$ [Fig. 4(b)] can be linked to a ~50 K gap. This, along with the suppression of χ starting ~55 K, seems to show singlet formation, with an energy scale of $\Delta_1 \simeq J \simeq \theta_W \simeq 50$ K and is consistent with a broad peak in the inelastic neutron scattering spectra of Nakatsuji *et al.*, which was attributed to the formation of short-range singlets on hexagonal motifs [14]. However, that drop in relaxation is quickly overtaken by appreciable low energy fluctuations giving a largely temperature independent relaxation from 5 to 20 K. This quasiplateau in $1/T_1$ is likely related to the continuum seen in inelastic neutron scattering [14].

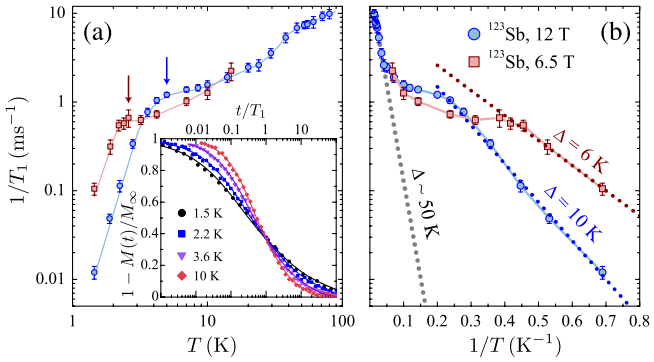

FIG. 4 (color online). (a) ^{123}Sb spin-lattice relaxation rate, $1/T_1(T)$, taken at 6.5 and 12 T. (b) Semilog plot of $1/T_1$ vs $1/T$ showing gapped behavior at low temperature, with $\Delta \simeq 6$ K at 6.5 T and $\Delta \simeq 10$ K at 12 T. Inset: the recovery curves $M(t)$ at selected temperatures showing a broadening distribution of relaxation times at low T, that is, nonetheless, small relative to the orders of magnitude drop in $1/T_1$.

There is another, important energy scale that is driven by the applied field. Below the quasiplateau, a crossover to an exponential drop occurs, indicating a true gap to magnetic excitations rather than the partial dimerization at ~50 K. The crossover temperature, T_C, is found to be roughly proportional to the applied field: $T_C \simeq 5$ K at 12 T and $T_C \simeq 2.6$ K at 6.5 T. The inset of Fig. 4 shows the expected T-dependence, $1/T_1 \propto \exp(-\Delta_0/T)$, of gapped excitations and a field-dependent gap $\Delta_0(H)$. At 12 T, $\Delta_0 \simeq 10$ K and at 6.5 T, $\Delta_0 \simeq 6$ K. The T_1 recovery curves (inset of Fig. 4), show that below ~10 K, the distribution of relaxation times widens appreciably, suggesting that there is, in fact, a distribution of gaps, as might be seen in a RSS [30].

This behavior runs contrary to the case of a standard gapped dimer state or a gapped QSL where a magnetic field closes the energy gap and eventually leads to magnetic order and power-law behavior [31,32]. It is also surprising given the $C(T)$ of Zhou *et al.* [6] which (after subtraction of Schottky anomalies) is very small but linear in the low-T limit and field-independent to as high as 9 T. This is difficult to reconcile with our observation of a clear gap to magnetic excitations, although a theoretical model supporting such a dichotomy between $C \propto T$ and exponential $1/T_1$ has been proposed for the related $S = 1$ system $Ba_3NiSb_2O_9$ [8].

On the basis of the structural and orbital information obtained by Nakatsuji *et al.*, two main scenarios for $Ba_3CuSb_2O_9$ have been suggested [14,15]: (1) A dynamical JT distortion that allows the system to maintain isotropic character may lead to an exotic spin-orbital liquid state with gapless excitations; (2) a disordered static JT distortion may occur that stabilizes a RSS. The configuration of distortions was proposed to obey locally a threefold rotation axis, with three dimers around a hexagon of Cu atoms.

If the first scenario is correct, the gap seen in $1/T_1$ likely represents a transition to a frozen state with gapped magnons. Indeed our $1/T_1$ results show qualitative similarities to the relaxation in other gapless QSL candidates [32–35] which exhibit field-induced phases with steep power law or exponential $1/T_1(T)$. In all cases, the change in dynamics is a smooth crossover, with no peak in $1/T_1$, atypical of standard phase transitions. A freezing of spins should be accompanied by a change in linewidth, but in this instance, it is difficult to distinguish between defect induced broadening and signs of freezing. Much of the increase in linewidth (Fig. 3) is occurring well above the crossover temperature ($\simeq 5$ K at 12 T) and is likely related to the defect contribution in χ_{macro}.

However, the QSL scenario (1) is put in doubt by strong evidence of dimerization occurring at ~55 K, as high as the exchange energy J. This is atypical of QSL phenomenology, where gaps are either absent or much smaller than J [36], and more befitting of an unfrustrated dimer system [37]. Given our T_1 and χ_{int} results, a more likely scenario is a type of RSS (2) with an energy gap of $\Delta_1 \sim 50$ K. As proposed by Nakatsuji *et al.* [14], this RSS consists largely of short-range singlets and our work is not consistent with a state involving arbitrarily long-range singlets [38] that would result in a finite susceptibility at low T.

Clearly, however, there remains a continuum of excitations below Δ_1 and the field-induced gap Δ_0 is much smaller. Similarity of the field-dependent gap size, $\Delta_0/H \sim 0.8$ K/T, with the Zeeman energy for an isolated $S = 1/2$ moment, $E_Z/H \simeq 1.34$ K/T, leads us to propose that it may be the weakly interacting defect spins that give rise to low-energy excitations in zero field and that freeze out as the defects are saturated with an applied magnetic field. Specific heat measurements are consistent with this picture, showing Schottky anomalies that shift to higher T with applied field [6,14].

The effect of these defect spins on the Sb nuclei is likely indirect since no shift is seen at low T and the relaxation in the plateau regime is too fast to be coming from distant spins. With a weak coupling between defects, so $\theta_{\text{def}} \simeq -0.5$ K, these defects would be slowly fluctuating, but even so, if they are coupled to the nuclei with the dipolar interaction, $1/T_1$ would be an order of magnitude smaller than what is seen. It is therefore more likely that they are distributed defects that cause a staggered magnetization or spin texture which is then strongly coupled to the Sb nuclei. As such, the spin textures contribute heavily to the NMR linewidth, but negligibly to K. This is commonplace in frustrated [25,27] and gapped quantum spin systems [39]. The precise nature of defects and resulting spin textures remains difficult to assess but they likely result from the out-of-plane Cu′ site which is linked to the honeycomb motifs by a frustrated isosceles triangle (see the structure in Ref. [14]). The Cu′ spins should be strongly coupled to the lattice [14], but may become unconstrained and easily saturated under applied field as the lattice becomes dimerized at low temperatures.

To conclude, we have performed local probe measurements on the $S = 1/2$ honeycomb system $Ba_3CuSb_2O_9$, revealing an exotic nonmagnetic state in zero field with dimerization occurring at 50 K and a lower temperature field-induced gap to magnetic excitations. Our measurements primarily support a RSS with low-energy excitations resulting from defect-induced spin textures that can be saturated with magnetic fields. This work allows us to distinguish between two proposed [14,15] orbital scenarios and likely implies random but static JT distortions. Within this new context of short range honeycomb structural order and orbital degrees of freedom, it would be enlightening to similarly investigate the $S = 1$ equivalent $Ba_3NiSb_2O_9$ which also may show a dynamic ground state [7] but may not be JT active.

We acknowledge useful discussions with O. Cépas, S. Nakatsuji, O. Motrunich, P. Deniard, T. McQueen, A. Amato, M. Bosiočić, and S. Johnston. Thanks also to D. Dragoe for ICP analysis of our samples. This work was partly supported by the EC FP 6 program, Contract No. RII3-CT-2003-505925 and Grant No. ANR-09-JCJC-0093-01. J. Q. acknowledges the financial support of the National Science and Engineering Research Council of Canada (NSERC).

[1] P. Mendels, F. Bert, M. A. de Vries, A. Olariu, A. Harrison, F. Duc, J. C. Trombe, J. S. Lord, A. Amato, and C. Baines, Phys. Rev. Lett. **98**, 077204 (2007).
[2] J. Helton *et al.*, Phys. Rev. Lett. **98**, 107204 (2007).
[3] Y. Okamoto, M. Nohara, H. Aruga-Katori, and H. Takagi, Phys. Rev. Lett. **99**, 137207 (2007).
[4] Y. Shimizu, K. Miyagawa, K. Kanoda, M. Maesato, and G. Saito, Phys. Rev. Lett. **91**, 107001 (2003).
[5] T. Itou, A. Oyamada, S. Maegawa, M. Tamura, and R. Kato, Phys. Rev. B **77**, 104413 (2008).
[6] H. Zhou, E. S. Choi, G. Li, L. Balicas, C. R. Wiebe, Y. Qiu, J. R. D. Copley, and J. S. Gardner, Phys. Rev. Lett. **106**, 147204 (2011).
[7] J. G. Cheng, G. Li, L. Balicas, J. S. Zhou, J. B. Goodenough, C. Xu, and H. D. Zhou, Phys. Rev. Lett. **107**, 197204 (2011).
[8] M. Serbyn, T. Senthil, and P. A. Lee, Phys. Rev. B **84**, 180403(R) (2011).
[9] C. Xu, F. Wang, Y. Qi, L. Balents, and M. P. A. Fisher, Phys. Rev. Lett. **108**, 087204 (2012).
[10] P. Rubin, A. Sherman, and M. Schreiber, Phys. Lett. A **376**, 1062 (2012).
[11] G. Chen, M. Hermele, and L. Radzihovsky, Phys. Rev. Lett. **109**, 016402 (2012).
[12] L. Thompson and P. A. Lee, arXiv:1202.5655.
[13] V. P. Köhl, Z. Anorg. Allg. Chem. **442**, 280 (1978).
[14] S. Nakatsuji *et al.*, Science **336**, 559 (2012).
[15] L. Balents, Science **336**, 547 (2012).

[16] See Supplemental Material at http://link.aps.org/supplemental/10.1103/PhysRevLett.109.117203 for details of sample growth and characterization, high-field magnetization measurements and spin-lattice relaxation measurements..
[17] A small, ~4%, quickly relaxing contribution to the μSR asymmetry is seen at all temperatures and has been subtracted. This is likely a small ferromagnetic impurity phase which is also seen in low-field susceptibility measurements.
[18] A conservative upper bound on the size of a possible frozen moment of $8 \times 10^{-4} \mu_B$ may be obtained by assuming the change in muon depolarization between 10 K and 20 mK is a result of static magnetism.
[19] E. Kermarrec, P. Mendels, F. Bert, R. H. Colman, A. S. Wills, P. Strobel, P. Bonville, A. Hillier, and A. Amato, Phys. Rev. B **84**, 100401(R) (2011).
[20] N. Elstner, R. R. P. Singh, and A. P. Young, Phys. Rev. Lett. **71**, 1629 (1993).
[21] S.-S. Lee and P. A. Lee, Phys. Rev. Lett. **95**, 036403 (2005).
[22] O. I. Motrunich, Phys. Rev. B **72**, 045105 (2005).
[23] P. Schiffer and I. Daruka, Phys. Rev. B **56**, 13712 (1997).; P. Mendels, A. Keren, L. Limot, M. Mekata, G. Collin, and M. Horvatić, Phys. Rev. Lett. **85**, 3496 (2000); L. Limot, P. Mendels, G. Collin, C. Mondelli, B. Ouladdiaf, H. Mutka, N. Blanchard, and M. Mekata, Phys. Rev. B **65**, 144447 (2002).
[24] F. Bert, S. Nakamae, F. Ladieu, D. L'Hôte, P. Bonville, F. Duc, J.-C. Trombe, and P. Mendels, Phys. Rev. B **76**, 132411 (2007).
[25] A. Olariu, P. Mendels, F. Bert, F. Duc, J. C. Trombe, M. A. de Vries, and A. Harrison, Phys. Rev. Lett. **100**, 087202 (2008).
[26] Y. Okamoto, H. Yoshida, and Z. Hiroi, J. Phys. Soc. Jpn. **78**, 033701 (2009).
[27] J. A. Quilliam, F. Bert, R. H. Colman, D. Boldrin, A. S. Wills, and P. Mendels, Phys. Rev. B **84**, 180401(R) (2011).
[28] C. Lacroix, P. Mendels, and F. Mila, *Introduction to Frustrated Magnetism* (Springer, New York, 2010).
[29] A. Suter, M. Mali, J. Roos, and D. Brinkmann, J. Phys. Condens. Matter **10**, 5977 (1998).
[30] T. Shiroka, F. Casola, V. Glazkov, A. Zheludev, K. Prša, H.-R. Ott, and J. Mesot, Phys. Rev. Lett. **106**, 137202 (2011).
[31] T. Giamarchi, C. Ruegg, and O. Tchernyshyov, Nature Phys. **4**, 198 (2008).
[32] F. L. Pratt, P. J. Baker, S. J. Blundell, T. Lancaster, S. Ohira-Kawamura, C. Baines, Y. Shimizu, K. Kanoda, I. Watanabe, and G. Saito, Nature (London) **471**, 612 (2011).
[33] M. Jeong, F. Bert, P. Mendels, F. Duc, J. C. Trombe, M. A. de Vries, and A. Harrison, Phys. Rev. Lett. **107**, 237201 (2011).
[34] Y. Shimizu, K. Miyagawa, K. Kanoda, M. Maesato, and G. Saito, Phys. Rev. B **73**, 140407(R) (2006).
[35] T. Itou, A. Oyamada, S. Maegawa, and R. Kato, Nature Phys. **6**, 673 (2010).
[36] S. Yan, D. A. Huse, and S. R. White, Science **332**, 1173 (2011).
[37] Y. Sasago, K. Uchinokura, A. Zheludev, and G. Shirane, Phys. Rev. B **55**, 8357 (1997).
[38] D. S. Fisher, Phys. Rev. B **50**, 3799 (1994).
[39] L. K. Alexander, J. Bobroff, A. V. Mahajan, B. Koteswararao, N. Laflorencie, and F. Alet, Phys. Rev. B **81**, 054438 (2010).